HHS Public Access

Author manuscript

Toxicol Lett. Author manuscript; available in PMC 2019 May 15.

Published in final edited form as:

Toxicol Lett. 2017 September 05; 279: 60–66. doi:10.1016/j.toxlet.2017.07.897.

Genotoxicity induced by monomethylarsonous acid (MMA^{+3}) in mouse thymic developing T cells

Huan Xu[a], **Sebastian Medina**[a], **Fredine T. Lauer**[a], **Christelle Douillet**[b], **Ke Jian Liu**[a], **Miroslav Stýblo**[b], and **Scott W. Burchiel**[a,*]

[a]The University of New Mexico College of Pharmacy, Department of Pharmaceutical Sciences, Albuquerque, NM 87131, United States

[b]Department of Nutrition, Gillings School of Global Public Health, University of North Carolina at Chapel Hill, Chapel Hill, NC 27516, United States

Abstract

Drinking water exposure to arsenic is known to cause immunotoxicity. Our previous studies demonstrated that monomethylarsonous acid (MMA^{+3}) was the major arsenical species presented in mouse thymus cells after a 30 d drinking water exposure to arsenite (As^{+3}). MMA^{+3} was also showed to be ten times more toxic than As^{+3} on the suppression of IL-7/STAT5 signaling in the double negative (DN) thymic T cells. In order to examine the genotoxicity induced by low to moderate doses of MMA^{+3}, isolated mouse thymus cells were treated with 5, 50 and 500 nM MMA^{+3} for 18 h *in vitro*. MMA^{+3} suppressed the proliferation of thymus cells in a dose dependent manner. MMA^{+3} at 5 nM induced DNA damage in DN not double positive (DP) cells. Differential sensitivity to double strand breaks and reactive oxygen species generation was noticed between DN and DP cells at 50 nM, but the effects were not seen at the high dose (500 nM). A stronger apoptotic effect induced by MMA^{+3} was noticed in DN cells than DP cells at low doses (5 and 50 nM), which was negated by the strong apoptosis induction at the high dose (500 nM). Analysis of intracellular MMA^{+3} concentrations in DN and DP cells, revealed that more MMA^{+3} accumulated in the DN cells after the *in vitro* treatment. Collectively, these results suggested that MMA^{+3} could directly induce strong genotoxicity in the early developing T cells in the thymus. The DN cells were much more sensitive to MMA^{+3} induced genotoxicity and apoptosis than DP cells, probably due to the higher intracellular levels of MMA^{+3}.

Keywords

Monomethylarsonous acid; Genotoxicity; Double negative T cells; Double positive T cells; Differential sensitivity; Apoptosis

*Corresponding author. sburchiel@salud.unm.edu, sburchiel@comcast.net (S.W. Burchiel).

Conflict of interest

None.

1. Introduction

Arsenic contamination in food and drinking water is a world-wide public health issue. It is known that arsenic exposure is associated with diseases such as skin lesions, diabetes, cardiovascular diseases, and cancers (Ahmed et al., 2014; Argos et al., 2010; Schuhmacher-Wolz et al., 2009; Vahter, 2008). Trivalent inorganic arsenic (arsenite, As^{+3}) is an environmentally prevalent form that is present in many water sources worldwide. As^{+3} is metabolized into mono-methylated and di-methylated trivalent and pentavalent species (Hughes et al., 2005). MMA^{+3} is an intermediate metabolic form of arsenic for the *in vivo* metabolic pathway. MMA^{+3} can be further metabolized to dimethy-larsonous acid (DMA^{+3}) and dimethylarsinic acid (DMA^{+5}) to be excluded from the body via urination. Previous *in vivo* and *in vitro* studies indicated that monomethylarsonous acid (MMA^{+3})was the most toxic form among arsenical species (Petrick et al., 2001; Styblo et al., 2000). We also found that MMA^{+3} accumulated in the primary immune organs, such as the thymus and bone marrow, in As^{+3} drinking water exposed mice (Xu et al., 2016a).

T cells are generated in bone marrow and got transferred into thymus for maturation. T cells are differentiated from double negative (DN, CD4−CD8−) stage to double positive (DP, CD4+ CD8+) stage, and then committed to either CD4+ single positive cells (CD4SP, T helper cells) or CD8+ single positive cells (CD8SP, cytotoxic T cells). IL-7 is an essential cytokine for thymopoiesis and early DN T cells are responsive to IL-7 induced proliferation and cell cycle progression (Gao et al., 2015). Previous studies indicated that arsenic exposure induced thymus atrophy, increased thymic cell apoptosis, and inhibited T cell development in humans and animal models after arsenic exposure (Ahmed et al., 2012; Raqib et al., 2009; Schulz et al., 2002). Studies in our laboratory indicated that the early developing T cells in the thymus are very sensitive to arsenic-induced toxicity. We found that As^{+3} induced genotoxicity and suppressed IL-7/STAT5 signaling pathways in the DN cells (Xu et al., 2016b, 2016c). DN cells were also shown to be more sensitive to As^{+3} induced genotoxicity than DP cells, due to the lack of As^{+3} efflux exporters and resultant higher intracellular As^{+3} accumulation (Xu et al., 2017). While there are several studies addressing the genotoxicity and non-genotoxicity induced by As^{+3} in thymus cells, studies on the thymic toxicity induced by MMA^{+3}, the most toxic and abundant arsenic metabolite *in vivo* in the thymus, have not been reported.

Our previous studies demonstrated that MMA^{+3} reduced the expression of cell cycle genes in early primary B and T cells (Ezeh et al., 2016; Xu et al., 2016c). Based on our recent findings that MMA^{+3} is the most abundant form of arsenic in the thymus cells in As^{+3} drinking water exposed mice (Xu et al., 2016a), *in vitro* studies using low to moderate concentrations of MMA^{+3} would be a better reflection of the direct thymic toxicity. In the present study, the genotoxicity induced by MMA^{+3} in the early DN and DP thymic T cells was analyzed and compared. The intracellular MMA^{+3} levels in the DN and DP cells after *in vitro* exposures were also examined.

2. Methods

2.1. Chemicals and reagents

Monomethylarsonous acid (MMA^{+3}, CAS 25400–23-1, CH_5AsO_2, > 99% purity analyzed independently by HG-CT-ICP-MS) was purchased from Toronto Research Chemicals (Toronto, Ontario, Canada). Dulbecco's phosphate buffered saline w/o Ca^{+2} or Mg^{+2} (DPBS $^{-}$) was purchased from Mediatech (Manassas, VA). Penicillin/ Streptomycin (Pen/Strep) and L-Glutamine were purchased from Life Technologies (Grand Island, NY). Fetal Bovine Serum (FBS) was purchased from Atlanta Biologicals (Flowery Branch, GA). Roswell Park Memorial Institute (RPMI) 1640 medium and Dimethyl sulfoxide (DMSO) were purchased from Sigma-Aldrich (St. Louis, MO). Recombinant murine IL-7 (Cat. No. 217–17) was purchased from Peprotech (Rocky Hill, NJ). Hanks Balanced Salt Solution (HBSS) was purchased from Lonza (Walkersville, MD). Sodium Hydroxide (NaOH) was purchased from EMD Chemicals Inc. (Gibbstown, NJ).The 0.5 M EDTA solution was purchased from Promega (Madison, WI). The Comet Assay kit (Cat. No. 4252–040-ESK) was purchased from Trevigen (Gaithersburg, MD). Cellometer acridine orange/propidium iodide (AO/PI) staining solution (Cat. No. CS2–0106-5ML) was purchased from Nexcelom Bioscience (Manchester, UK). FITC rat anti-mouse CD8a (Cat. No.553031), PE rat anti-mouse CD8 (Cat. No.553033), PE rat anti-mouse CD4 (Cat. No. 553730), APC rat anti-mouse CD4 (Cat. No.553051), PerCP-Cy™5.5 Mouse Anti-H2AX (pS139) (Cat. No. 564718) antibodies, FITC Annexin V Apoptosis Detection Kit I (Cat.No. 556547) and 7-Amino-Actinomycin D (7-AAD) (Cat. No. 559925) were purchased from BD Biosciences (San Jose, CA).EBioscience™ IC Fixation Buffer (Cat. No. 00–8222-49), Invitrogen™ SYBR™ Gold Nucleic Acid Gel Stain (Cat. No. S11494) and Dihydroethidium (DHE, Cat. No. D11347) were purchased from Thermo Fisher Scientific (Waltham, MA). EasySep™ PE positive selection kit (Cat. No. 18557) was purchased from STEMCELL Technologies (Vancouver, BC, Canada). EDTA (0.5 M) and CellTiter 96® AQ_{ueous} One Solution Cell Proliferation Assay (Cat. No. G3580) were purchased from Promega (Madison, WI).

2.2. Isolation of primary mouse thymus cells

C57BL/6J male mice were purchased at 8 weeks of age from Jackson Laboratory (Bar Harbor, ME). All animal experiments were performed following the protocols approved by the Institutional Animal Use and Care Committee at the University of New Mexico Health Sciences Center. Following 2 week of acclimations in the animal facility, mice were sacrificed and thymus cells were isolated following sterile procedures described in Xu et al. (2016c). Basically, the thymuses from male C57BL/6J mice were harvested in our animal facility and transferred to our laboratory in HBSS on ice. Single cell suspension of thymus cells were prepared by homogenizing the organ between the frosted ends of two sterilized microscope slides (Fisher Scientific, Pittsburgh, PA) into a dish containing 10 mL of cold mouse medium (500 ml RPMI 1640 supplemented with 10% FBS, 2 mM L-glutamine, and 100 U/ml Pen/Strep). Cells were centrifuged at 200 × *g* for 10 min, aspirated, and washed with cold mouse medium. The cell count and viability were determined by AO/PI staining on a Nexcelom Cellometer 2000. Thymus cells from three mice were pooled and treated with MMA^{+3} *in vitro* in each single experiment.

2.3. Cell proliferation assay (MTS assay)

Thymus cells were seeded at 1×10^6 cells/mL into 24-well plates in mouse medium with or without 50 ng/mL IL-7, and treated with MMA^{+3} for 18 h *in vitro*. One hundred microliter of cells were transferred into a 96-well flat bottom plate and mixed with 20 μl of CellTiter 96® AQ_{ueous} One Solution Reagent. The plate was incubated at 37 °C for 4 h and read on a SpectraMax® 340PC microplate reader (Molecular Devices, Sunnyvale, CA) at 490 nm wavelength to measure the formation of formazan. Three wells of medium without any cells were used in the experiment to measure the assay background absorbance, which was subtracted from the absorbance of the samples.

2.4. DN cell enrichment and thymus cell sorting

The cell enrichment and sorting procedures were developed to ensure the appropriate yield of DN cells for our experiment as previously described in Xu et al. (2017). Basically, an aliquot (~1.5×10^8 cells in 6 mL) of the isolated thymus cells were centrifuged and concentrated to 1×10^8 cells/mL in mouse medium and stained with 1 μg/mL PE-conjugated anti-CD4 and PE-conjugated anti-CD8 antibodies for 15 min at RT in dark. 150 μl of PE selection cocktail was then added to the cell suspension, followed by a15 min RT incubation. Seventy five microliter of magnetic nanoparticles was added to the cell suspension and mixed well. After a 10 min RT incubation, cell suspension volume was brought up to 2.5 mL by adding $DPBS^-$ containing 2% FBS and 1 mM EDTA. Tubes were then placed into the EasySep™ magnet (STEMCELL Technologies) for 5 min and cells that remained in suspension (~ 94% pure DN cells) were collected into a new tube. Enriched DN cell suspension and the remaining total thymus cells were stained with 2 μg/mL FITC-conjugated anti-CD8 and APC-conjugated anti-CD4 in mouse medium and DN and DP cell populations were sorted into two 15 mL tubes on an iCyt SY3200 cell sorter (Sony, San Jose, CA) at 15,000 events/s to achieve > 99% purity. By adding the above described enrichment step before cell sorting, the efficiency of obtaining DN cells was significantly improved.

2.5. Comet assay (Single cell gel electrophoresis assay)

MMA^{+3} treated DN and DP cells were immobilized in low melting point agarose on a Trevigen CometSlide™ according to the Comet assay kit instructions. Immobilized cells were lysed with Lysis Solution with 10% DMSO overnight. On the next day, DNA in the lysed cells was unwound with basic pH buffer (8 g NaOH with 2 mL of 0.5 M EDTA in 1 L of deionized water, pH > 13) at RT for 45 min. After the unwinding step, slides were electrophoresed in ice cold basic buffer in CometAssay® Electrophoresis System II (Trevigen) at 21 V for 30 min. Slides were then washed, dried and stained with Sybr Gold (1:10000 dilution in TE buffer) and imaged using an epifluorescence microscope. Fifty randomly selected cells from each well were scored using CometScore software (TriTek Corp., Sumerduck, VA). DNA damage was reported by percentage of DNA in tail (Collins, 2004).

2.6. Flow cytometry analysis

For ROS detection, DHE was resuspended with 158 μl DMSO, and diluted to a final concentration of 5 μM in $DPBS^{-}$. One million MMA^{+3} treated primary thymus cells were washed with $DPBS^{-}$ and stained with 0.25 μg of FITC CD8 and APC CD4 antibody at 37 °C in 100 μl of 5 μM DHE solution for 30 min. Cells were then washed twice with $DPBS^{-}$ and analyzed on an AccuriC6 Flow Analyzer (BD Biosciences). 20,000 events were collected for each sample and the mean channel fluorescence in FL2 (488 nm blue laser, 585/40 standard filter) was used as DHE fluorescence intensity.

For detection of DNA double strand breaks (DSBs), 1×10^6 MMA^{+3} treated primary thymus cells were washed twice with $DPBS^{-}$ and stained with 0.25 μg of FITC CD8 and APC CD4 antibody at RT in 100 μl $DPBS^{-}$ for 30 min in the dark. Cells were then fixed by adding 100 μl of IC fixation buffer and incubated for 15 min at RT in the dark. Following incubation, cells were washed twice with $DPBS^{-}$ and incubated in 200 μl of 90% ice cold methanol for 15 min 4 °C in the dark. After two washes with $DPBS^{-}$, cells were resuspended in 100 μl of $DPBS^{-}$ and stained with 0.5 μg of PerCP-Cy™ 5.5 anti-γ-H2AX (pS139) or isotype control and incubated for 30 min at RT in dark. Washed cells were analyzed on an AccuriC6 Flow Analyzer.

For the detection of apoptosis, 5×10^5 thymus cells were resuspended in 100 μl 1 X Annexin V Binding Buffer and stained with 5 μl of FITC Annexin V, 5 μl of 7-AAD Staining Solution, 0.25 μg of PE CD8 and APC CD4 antibodies for 15 min at RT in dark. Four hundred microliter of 1 X Annexin V Binding Buffer was added to the samples before analyzing on an AccuriC6 Flow Analyzer. Primary thymus cells treated with 50 μM Etoposide for 1 h were used as positive control.

2.7. Oxidation state specific hydride generation-cryotrapping-inductively coupled plasma-mass spectrometry (HG-CT-ICP-MS)

The intracellular levels of trivalent and pentavalent arsenic species were analyzed by HG-CT-ICP-MS as previously described (Currier et al., 2014; Matoušek et al., 2013). Briefly, cell pellets were lysed in ice-cold deionized water. The trivalent species were measured in an aliquot of cell lysate directly, without any pretreatment. Another aliquot was treated with 2% cysteine and analyzed for total inorganic arsenic, total mono-methylated arsenic, and total di-methylated arsenic. Calibration curves were generated using cysteine-treated pentavalent arsenic standards as previously described (Hernández-Zavala et al., 2008). The concentrations of pentavalent arsenic species were determined as a difference between the values obtained for cysteine-treated aliquots and values from untreated sample aliquots. The instrumental lower limit of detection for arsenic species analyzed by HG-CT-ICP-MS ranged from 0.04 pg for methylated arsenicals to 2.0 pg for inorganic arsenicals. All values are reported as pg of arsenic in an arsenic species.

2.8. Statistics

Data were analyzed with Excel 2010 and Sigma Plot v12.5 software. One-way analysis of variance (ANOVA) and Dunnett's *t*-test were used to determine differences between the

control (Cont) and treatment groups. Three independent experiments (n = 3) were performed and analyzed for each dose of MMA^{+3}.

3. Results

3.1. MMA^{+3} inhibited the proliferation of mouse thymus cells

Our previous studies indicated that MMA^{+3} was the major arsenic species present in the mouse thymus cells after 30 d As^{+3} drinking water exposure (Xu et al., 2016a). We also showed that 18 h *in vitro* treatment of MMA^{+3} could suppress cell cycle gene expression in DN T cells through the inhibition of IL-7/STAT5 signaling (Xu et al., 2016c). In order to determine if MMA^{+3} inhibits the proliferation of thymus cells, primary thymus cells were isolated from male C57BL/6J mice at 10–14 weeks age and were treated with 5, 50 and 500 nM MMA^{+3} for 18 h *in vitro* in the medium with or without 50 ng/mL IL-7. While IL-7 significantly increased the proliferation of the thymus cells, MMA^{+3} dose-dependently inhibited the proliferation starting from 5 nM in cultures not treated with IL-7 and 50 nM in cultures with IL-7 (Fig. 1). The results demonstrated that low to moderate doses of MMA^{+3} could inhibit the proliferation of mouse thymus cells. Since IL-7 stimulated the proliferation of the thymus cells but did not reverse the inhibition caused by MMA^{+3}, other type of toxicities (genotoxicity, oxidative stress, *etc.*) than the IL-7 signaling suppression could also be involved in MMA^{+3} induced toxicity in mouse thymus cells.

3.2. MMA^{+3} induced differential DNA damage in DN and DP thymic T cells

Previous studies in our lab indicated that As^{+3} and MMA^{+3} induced significant DNA damage in mouse primary thymus cells (Xu et al., 2016a,b). To specifically examine the DNA damage induced by MMA^{+3} in DN and DP cells, the two immature thymic T cell populations with high proliferation potentials (DN and DP cells) were isolated from whole thymus cells using magnetic bead enrichment and cell sorting. A significant increase in DNA damage was observed in DN cells starting from 5 nM and DP cells starting from 50 nM after the 18 h MMA^{+3} *in vitro* treatment (Fig. 2A). Differential DNA damage between DN and DP cells was observed at 50 nM, which was not seen at the higher dose (500 nM).

Double strand breaks (DSBs) are the most cytotoxic form of DNA lesions, which can be assessed by an increase of γ-H2AX (Kuo and Yang, 2008). A significant increase in γ-H2AX was observed in DN cells treated with 50 nM MMA^{+3} for 18 h *in vitro*, but not in DP cells (Fig. 2B). The differential γ-H2AX increase also disappeared at 500 nM between the DN and DP cell populations, which may be related to the high cytotoxicity of MMA^{+3}.

3.3. MMA^{+3} induced differential increase of oxidative stress and apoptosis in DN and DP thymic T cells

Our previous studies demonstrated that DSBs induced by As^{+3} at 500 nM *in vitro* were related to an increase of ROS production (Xu et al., 2016b). With the observation of differential DNA damage and γ-H2AX increases in the DN and DP cells after MMA^{+3} 18 h *in vitro* treatment, DHE staining was performed to investigate the ROS production in these cells. Again, an increase of ROS was only observed in DN cells at 50 nM, and the loss of differential effects between DN and DP cells was seen at 500 nM (Fig. 3).

We have already shown that 500 nM MMA^{+3} had high toxicity *in vitro* to pre-B cells (Ezeh et al., 2014). Since we suspected that the loss of differential sensitivity to MMA^{+3} between the DN and DP cells at 500 nM was due to high cytotoxicity, an Annexin V/7-AAD staining apoptosis assay was performed on primary thymus cells treated with MMA^{+3} for 18 h *in vitro*. A dose-dependent decrease in viable cells (Annexin V−, 7-AAD−) and increase in late apoptotic cells (Annexin V+, 7-AAD+) were seen in the DN cell population starting at the 5 nM exposure (Fig. 4). While most of the DP cell population was in the early apoptotic stage at the high dose (500 nM), two times fewer DP cells were in the late apoptotic stage than the DN cells (Fig. 4C and D). Therefore, the DN cells were more sensitive to MMA^{+3} induced apoptotic effects than the DP cells.

3.4. Differential levels of intracellular MMA^{+3} accumulated by DN and DP thymic T cells in vitro

Our previous study indicated that As^{+3} induced more DNA damage in DN cells than in DP cells due to a higher intracellular accumulation of As^{+3} in DN cells. Based on the differential sensitivities to MMA^{+3} between DN and DP cells (DNA damage, oxidative stress and apoptosis), we suspected that DN cells may accumulate more intracellular MMA^{+3} than DP cells. Therefore, we analyzed the intracellular levels of MMA^{+3} in DN and DP cells after 18 h *in vitro* treatment of 5 and 50 nM MMA^{+3} using HG-CT-ICP-MS. More intracellular MMA^{+3} was found in both the 5 and 50 nM MMA^{+3} treated DN cells than DP cells (Fig. 5). These results suggest that intracellular accumulation and transportation of MMA^{+3} may be responsible for the high sensitivity of the DN cells to MMA^{+3} induced genotoxicity.

4. Discussion

It is known that arsenic exposures cause detrimental effects on many different types of cells and tissues (Argos et al., 2010; Biswas et al., 2008; Gonsebatt et al., 1994; Cooper et al., 2013; Soto-Peña et al., 2006). Our previous studies indicated that mouse thymus cells were sensitive to arsenic-induced genotoxicity both *in vitro* and *in vivo* (Xu et al., 2016a,b). The *in vivo* metabolite of the inorganic arsenical species in the environment, MMA^{+3}, was shown to be the most prevalent form of arsenic in mouse thymus cells after a 30 d drinking water exposure (Xu et al., 2016a). Lymphoid cells have limited or no capacity to form MMA^{+3} from As^{+3}, due to the lack of expression or activity of the enzyme AS3MT (Meza et al., 2007). Our unpublished observations also failed to find any AS3MT RNA or protein expression in mouse thymus cells, as well as a lack of MMA^{+3} formation following incubation with As^{+3}. The results from this study and other MMA^{+3} toxicity studies showed that MMA^{+3} was more toxic than As^{+3} in multiple types of cells (Ezeh et al., 2014; Petrick et al., 2001; Stýblo et al., 2002). Therefore, it is possible that MMA^{+3} is the major substance that induces the *in vivo* toxic effects in the thymus following As^{+3} exposure.

As^{+3} induces genotoxicity through the inhibition of DNA repair and generation of oxidative stress in thymus cells (Xu et al., 2016b). Low concentrations of As^{+3} at 50 nM were found to increase DNA damage in DN cells *in vitro*, and 500 nM As^{+3} was found to induce oxidative stress in DN cells. The DNA damage increase was also found to be related to the

inhibition of poly (ADP-ribose) polymerase activity (Ding et al., 2017; Xu et al., 2016b; Zhou et al., 2011). In the present study, we found that MMA^{+3} induced DNA damage at the 5 nM concentration and oxidative stress at 50 nM (Figs. 2 A and 3 B). Both concentrations were ten times lower than As^{+3} doses. The higher toxicity of MMA^{+3} compared to As^{+3} was consistent with our previous finding in IL-7/ STAT5 signaling inhibition in pre-B and DN T cells (Ezeh et al., 2016; Xu et al., 2016c). The *in vitro* doses we used in both studies were comparable to the thymic intracellular MMA^{+3} concentrations from the 30 d drinking water exposure (Xu et al., 2016b). Therefore, the early thymic T cells are more sensitive to MMA^{+3} induced both genotoxicity (DNA damage, DNA repair inhibition) and cell signaling inhibition (IL-7 signaling inhibition) at environmentally relevant low doses.

In our previous study, we did not find any apoptosis induced by As^{+3} at 500 nM in the DN cells (Xu et al., 2016b). However, MMA^{+3} at 5 nM started to induce apoptosis in the DN cells after 18 h *in vitro* treatment. 5 nM MMA^{+3} also caused a significant increase of late stage apoptotic cells in the DN cell population. Our previous results indicated that MMA^{+3} suppressed IL-7/STAT5 signaling and cell cycle gene expression at 50 nM (Xu et al., 2016b). Based on the findings that low dose MMA^{+3} induced the generation of DSBs and oxidative stress, and a higher accumulation of intracellular MMA^{+3} in DN cells compared to DP cells, it is very likely that the strong apoptotic effect of MMA^{+3} on DN cells is the result of the combined effects of genotoxicity, altered cell signaling, and MMA^{+3} transportation.

We found a differential sensitivity between DN and DP cells to As^{+3} induced genotoxicity, which was related to the limited ability to upregulate the As^{+3} efflux transporters (Mdr1 and Mrp1) and higher intracellular As^{+3} accumulation in the DN cells (Xu et al., 2017). In the present study, we found that intracellular retention of MMA^{+3} was also higher in DN cells than DP cells (Fig. 5). The differential retention of MMA^{+3} in DN and DP cells may also be related to the expression of MMA^{+3} transporters. Aquaporin 9 (AQP9) and Glucose transporter 2 (GLUT2) are the known transporters of trivalent methylated arsenical species (Maciaszczyk-Dziubinska et al., 2012). The differential intracellular accumulation of MMA^{+3} between DN and DP cells could be caused by the difference in the expression of these transporters. Also, since more transporters for MMA^{+3} in the mammalian system are still to be determined, future studies should be conducted to identify and compare the expression of MMA^{+3} transporters in different types of cells.

In summary, we found that low to moderate doses of MMA^{+3} suppressed the proliferation of mouse thymus cells. MMA^{+3} induced DNA damage, oxidative stress and apoptosis at lower doses than As^{+3}, specifically in early DN thymic T cells. The differential cellular accumulation of MMA^{+3} between DN and DP cells was also observed, which could be responsible for the differential sensitivity at the environmentally relevant doses. The intracellular concentrations of MMA^{+3} used in this *in vitro* study are comparable to the thymic intracellular MMA^{+3} concentrations we measured from low to moderate doses of *in vivo* 30 d As^{+3} drinking water exposures (Xu et al., 2016a). Thus, the MMA^{+3} plays an important role in thymic toxicity and alterations on T cell development related with arsenic exposure. Its differential toxicity in thymic cells subsets may be associated with the difference in accumulation on these cells.

Acknowledgments

Funding

This work was funded by National Institute of Environmental Health Sciences at the National Institutes of Health (grant number R01 ES019968).

References

Ahmed S, Ahsan KB, Kippler M, Mily A, Wagatsuma Y, Hoque AM, Ngom PT, El Arifeen S, Raqib R, Vahter M, 2012 In utero arsenic exposure is associated with impaired thymic function in newborns possibly via oxidative stress and apoptosis. Toxicol. Sci 129 (2), 305–314. [PubMed: 22713597]

Ahmed S, Moore SE, Kippler M, Gardner R, Hawlader MD, Wagatsuma Y, Raqib R, Vahter M, 2014 Arsenic exposure and cell-mediated immunity in pre-school children in rural Bangladesh. Toxicol. Sci 141 (1), 166–175. [PubMed: 24924402]

Argos M, Kalra T, Rathouz PJ, Chen Y, Pierce B, Parvez F, Islam T, Ahmed A, Rakibuz-Zaman M, Hasan R, Sarwar G, Slavkovich V, van Geen A, Graziano J, Ahsan H, 2010 Arsenic exposure from drinking water, and all-cause and chronic-disease mortalities in Bangladesh (HEALS): a prospective cohort study. Lancet 376 (9737), 252–258. [PubMed: 20646756]

Biswas R, Ghosh P, Banerjee N, Das JK, Sau T, Banerjee A, Roy S, Ganguly S, Chatterjee M, Mukherjee A, Giri AK, 2008 Analysis of T-cell proliferation and cytokine secretion in the individuals exposed to arsenic. Hum. Exp. Toxicol 27 (5), 381–386. [PubMed: 18715884]

Collins AR, 2004 The comet assay for DNA damage and repair: principles, applications, and limitations. Mol. Biotechnol 26 (3), 249–261. [PubMed: 15004294]

Cooper KL, King BS, Sandoval MM, Liu KJ, Hudson LG, 2013 Reduction of arsenite-enhanced ultraviolet radiation-induced DNA damage by supplemental zinc. Toxicol. Appl. Pharmacol 269, 81–88. [PubMed: 23523584]

Currier JM, Ishida MC, González-Horta C, Sánchez-Ramírez B, Ballinas-Casarrubias L, Gutiérrez-Torres DS, Cerón RH, Morales DV, Terrazas FA, Del Razo LM, García-Vargas GG, Saunders RJ, Drobná Z, Fry RC, Matoušek T, Buse JB, Mendez MA, Loomis D, Stýblo M, 2014 Associations between arsenic species in exfoliated urothelial cells and prevalence of diabetes among residents of Chihuahua, Mexico. Environ. Health Perspect 122 (10), 1088–1094. [PubMed: 25000461]

Ding X, Zhou X, Cooper KL, Huestis J, Hudson LG, Liu KJ, 2017 Differential sensitivities of cellular XPA and PARP-1 to arsenite inhibition and zinc rescue. Toxicol Appl. Pharmacol 10.1016/j.taap.2017.05.031. Advance online publication.

Ezeh PC, Lauer FT, MacKenzie D, McClain S, Liu KJ, Hudson LG, Gandolfi AJ, Burchiel SW, 2014 Arsenite selectively inhibits mouse bone marrow lymphoid progenitor cell development in vivo and in vitro and suppresses humoral immunity in vivo. PLoS One 9 (4), e93920. [PubMed: 24714590]

Ezeh PC, Xu H, Lauer FT, Liu KJ, Hudson LG, Burchiel SW, 2016 Monomethylarsonous acid (MMA + 3) inhibits IL-7 signaling in mouse pre-B cells. Toxicol. Sci 149 (2), 289–299. [PubMed: 26518055]

Gao J, Zhao L, Wan YY, Zhu B, 2015 Mechanism of action of IL-7 and its potential applications and limitations in cancer immunotherapy. Int. J. Mol. Sci 16 (5), 10267–10280. [PubMed: 25955647]

Gonsebatt ME, Vega L, Montero R, Garcia-Vargas G, Del Razo LM, Albores A, Cebrian ME, Ostrosky-Wegman P, 1994 Lymphocyte replicating ability in individuals exposed to arsenic via drinking water. Mutat. Res 313, 293–299. [PubMed: 7523914]

Hernández-Zavala A, Matoušek T, Drobná Z, Paul DS, Walton F, Adair BM, Jiří D, Thomas DJ, Stýblo M, 2008 Speciation analysis of arsenic in biological matrices by automated hydride generation-cryotrapping-atomic absorption spectrometry with multiple microflame quartz tube atomizer (multiatomizer). J. Anal. At. Spectrom 23, 342–351. [PubMed: 18677417]

Hughes MF, Devesa V, Adair BM, Styblo M, Kenyon EM, Thomas DJ, 2005 Tissue dosimetry, metabolism and excretion of pentavalent and trivalent monomethylated arsenic in mice after oral administration. Toxicol. Appl. Pharmacol 208 (2), 186–197. [PubMed: 16183392]

Kuo LJ, Yang LX, 2008 Gamma-H2AX – a novel biomarker for DNA double-strand breaks. In Vivo 22 (3), 305–309. [PubMed: 18610740]

Maciaszczyk-Dziubinska E, Wawrzycka D, Wysocki R, 2012 Arsenic and antimony transporters in eukaryotes. Int. J. Mol. Sci 13 (3), 3527–3548. [PubMed: 22489166]

Matoušek T, Currier JM, Trojánková N, Saunders RJ, Ishida MC, González-Horta C, Musil S, Mester Z, Stýblo M, Dědina J, 2013 Selective hydride generation-cryotrapping-ICP-MS for arsenic speciation analysis at picogram levels: analysis of river and sea water reference materials and human bladder epithelial cells. J. Anal. At. Spectrom 28 (9), 1456–1465. [PubMed: 24014931]

Meza M, Gandolfi AJ, Klimecki WT, 2007 Developmental and genetic modulation of arsenic biotransformation: a gene by environment interaction? Toxicol. Appl. Pharmacol 222 (3), 381–387. [PubMed: 17306849]

Petrick JS, Jagadish B, Mash EA, Aposhian HV, 2001 Monomethylarsonous acid (MMA(III)) and arsenite: LD(50) in hamsters and in vitro inhibition of pyruvate dehydrogenase. Chem. Res. Toxicol 14 (6), 651–656. [PubMed: 11409934]

Raqib R, Ahmed S, Sultana R, Wagatsuma Y, Mondal D, Hoque AM, Nermell B, Yunus M, Roy S, Persson LA, Arifeen SE, Moore S, Vahter M, 2009 Effects of in utero arsenic exposure on child immunity and morbidity in rural Bangladesh. Toxicol. Lett 185 (3), 197–202. [PubMed: 19167470]

Schuhmacher-Wolz U, Dieter HH, Klein D, Schneider K, 2009 Oral exposure to inorganic arsenic: evaluation of its carcinogenic and non-carcinogenic effects. Crit. Rev. Toxicol 39, 271–298. [PubMed: 19235533]

Schulz H, Nagymajtényi L, Institoris L, Papp A, Siroki O, 2002 A study on behavioral, neurotoxicological, and immunotoxicological effects of subchronic arsenic treatment in rats. J. Toxicol. Environ. Health A 65 (16), 1181–1193. [PubMed: 12167215]

Soto-Peña GA, Luna AL, Acosta-Saavedra L, Conde P, López-Carrillo L, Cebrián ME, Bastida M, Calderón-Aranda ES, Vega L, 2006 Assessment of lymphocyte subpopulations and cytokine secretion in children exposed to arsenic. FASEB J 20 (6), 779–781. [PubMed: 16461332]

Stýblo M, Drobná Z, Jaspers I, Lin S, Thomas DJ, 2002 The role of biomethylation in toxicity and carcinogenicity of arsenic: a research update. Environ. Health Perspect 767–771. [PubMed: 12426129]

Styblo M, Del Razo LM, Vega L, Germolec DR, LeCluyse EL, Hamilton GA, Reed W, Wang C, Cullen WR, Thomas DJ, 2000 Comparative toxicity of trivalent and pentavalent inorganic and methylated arsenicals in rat and human cells. Arch. Toxicol 74 (6), 289–299. [PubMed: 11005674]

Vahter M, 2008 Health effects of early life exposure to arsenic. Basic Clin. Pharmacol.Toxicol 102, 204–211. [PubMed: 18226075]

Xu H, McClain S, Medina S, Lauer FT, Liu KJ, Hudson LG, Stýblo M, Burchiel SW, 2016a Differential sensitivities of bone marrow, spleen and thymus to genotoxicity induced by environmentally relevant concentrations of arsenite. Toxicol. Lett 262, 55–61. [PubMed: 27659730]

Xu H, Zhou X, Wen X, Lauer FT, Liu KJ, Hudson LG, Aleksunes LM, Burchiel SW, 2016b Environmentally-relevant concentrations of arsenite induce dose-dependent differential genotoxicity through poly(ADP-ribose) polymerase (PARP) inhibition and oxidative stress in mouse thymus cells. Toxicol. Sci 149, 31–41. [PubMed: 26443841]

Xu H, Lauer FT, Liu KJ, Hudson LG, Burchiel SW, 2016c Environmentally relevant concentrations of arsenite and monomethylarsonous acid inhibit IL-7/STAT5 cytokine signaling pathways in mouse CD3 + CD4−CD8-double negative thymus cells. Toxicol. Lett 247, 62–68. [PubMed: 26921788]

Xu H, Medina S, Lauer FT, Douillet C, Liu KJ, Hudson LG, Stýblo M, Aleksunes LM, Burchiel SW, 2017 Efflux transporters regulate arsenite induced genotoxicity in double negative and double positive t cells. Toxicol. Sci 10.1093/toxsci/kfx075.

Zhou X, Sun X, Cooper KL, Wang F, Liu KJ, Hudson LG, 2011 Arsenite interacts selectively with zinc finger proteins containing C3H1 or C4 motifs. J. Biol. Chem 286 (26), 22855–22863. [PubMed: 21550982]

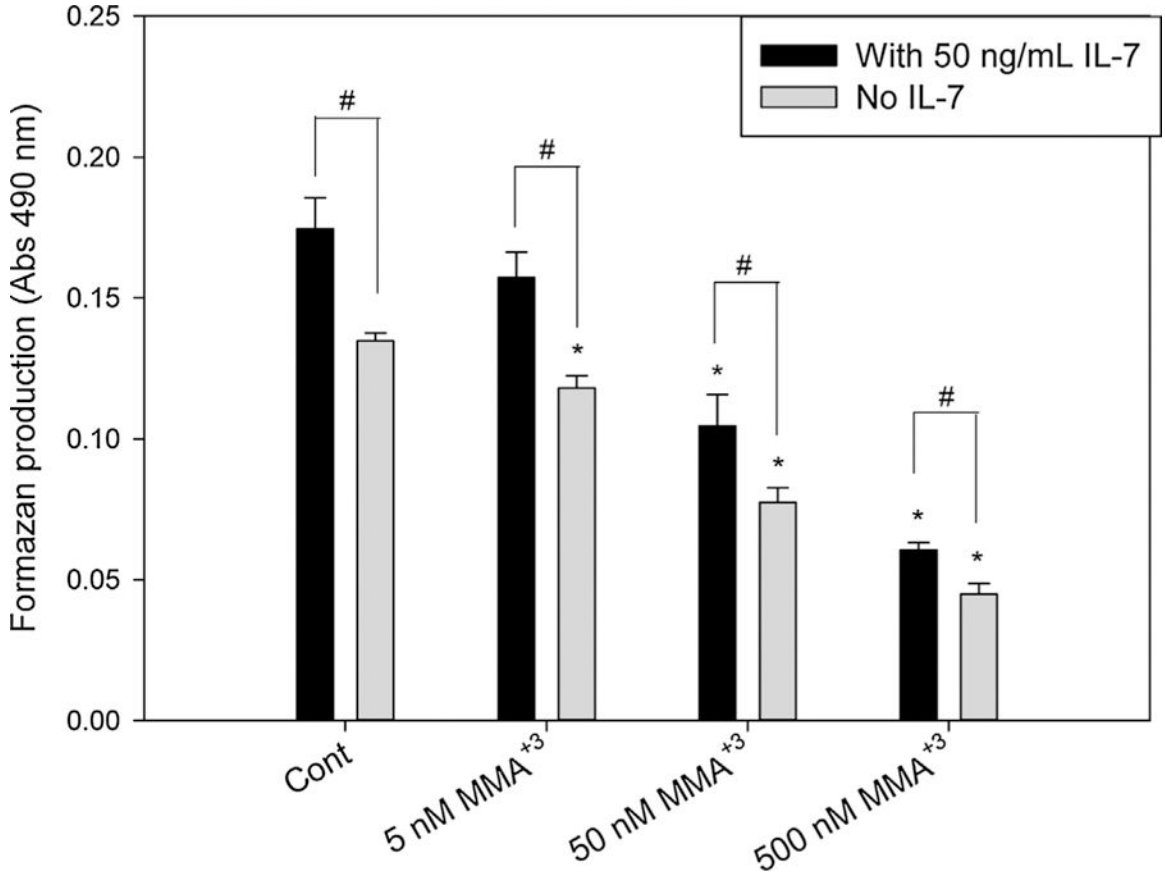

Fig. 1.

Proliferation of mouse primary thymus cells after exposure to 5, 50 and 500 nM MMA^{+3} for 18 h *in vitro* with/without IL-7.Isolated thymus cells were treated with MMA^{+3} in the medium with or without 50 ng/mL IL-7. The MTS assay used CellTiter 96® AQ_{ueous} One Solution Reagent to measure the proliferation. Formazan production from the cell culture was analyzed from the reading of absorbance at 490 nm. *Significantly different compared to Cont ($n = 3$, $p < 0.05$). # Significantly different compared to the same doses in the medium with 50 ng/mL IL-7 ($n = 3$, $p < 0.05$). Results are Means ± SD.

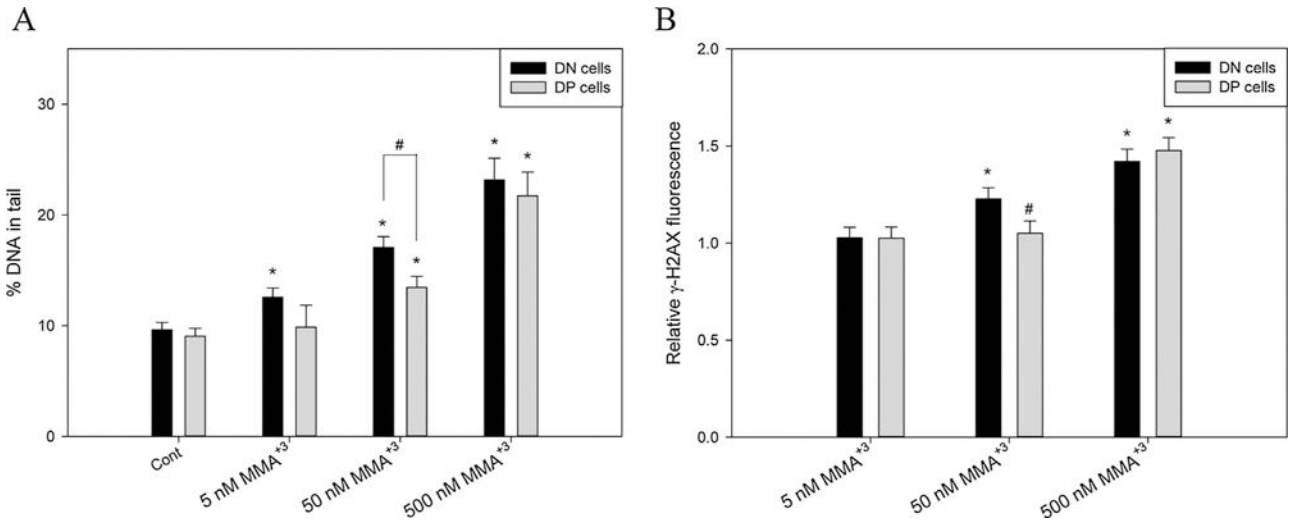

Fig. 2.

DNA damage and double strand breaks in DN and DP cells after exposure to 5, 50 and 500 nM MMA^{+3} for 18 h. DN and DP cells were treated with MMA^{+3} and analyzed by Comet assay or γ-H2AX intracellular flow cytometry. A, DNA damage in DN and DP cells. B, relative γ-H2AX fluorescence normalized to control. *Significantly different compared to Cont or the low dose (5 nM) ($n = 3$, $p < 0.05$). # Significantly different compared to the DN cells at the same dose ($n = 3$, $p < 0.05$). Results are Means ± SD.

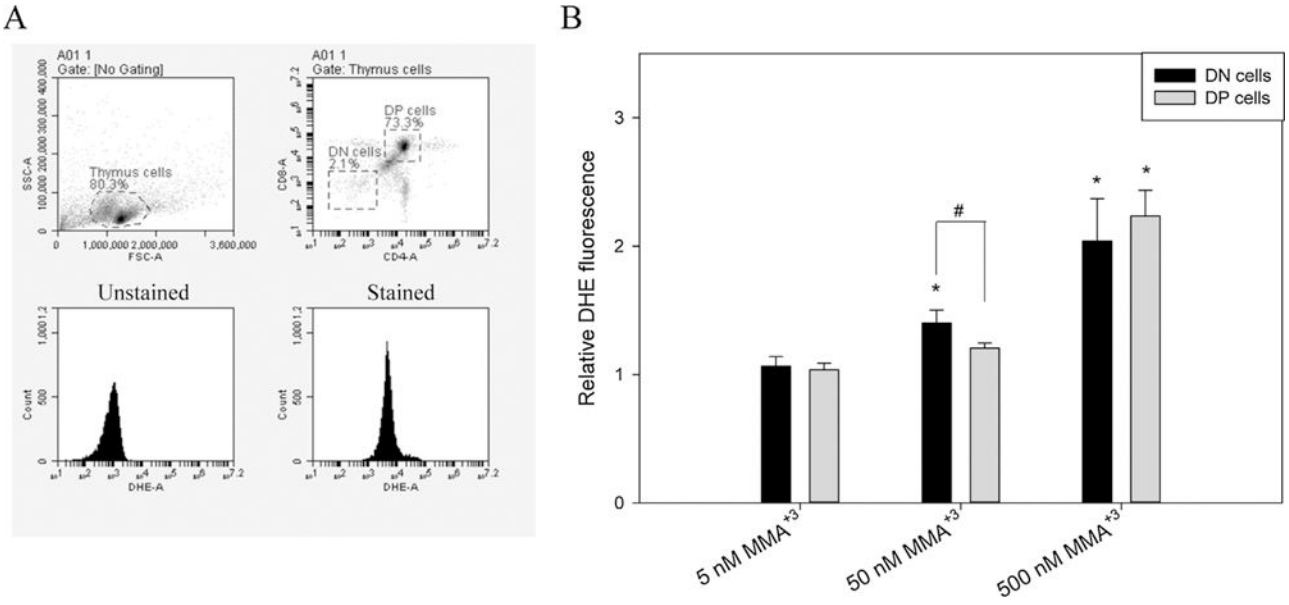

Fig. 3.

ROS production in DN and DP cells after exposure to 5, 50 and 500 nM MMA^{+3} for 18 h. Thymus cells were treated with MMA^{+3} and analyzed by CD4, CD8 cell surface markers and DHE staining. A, DN and DP cell gating and stained/unstained samples. B, relative DHE fluorescence normalized to control. *Significantly different compared to the low dose (5 nM) ($n = 3$, $p < 0.05$). # Significantly different compared to the DN cells at the same dose ($n = 3$, $p < 0.05$). Results are Means ± SD.

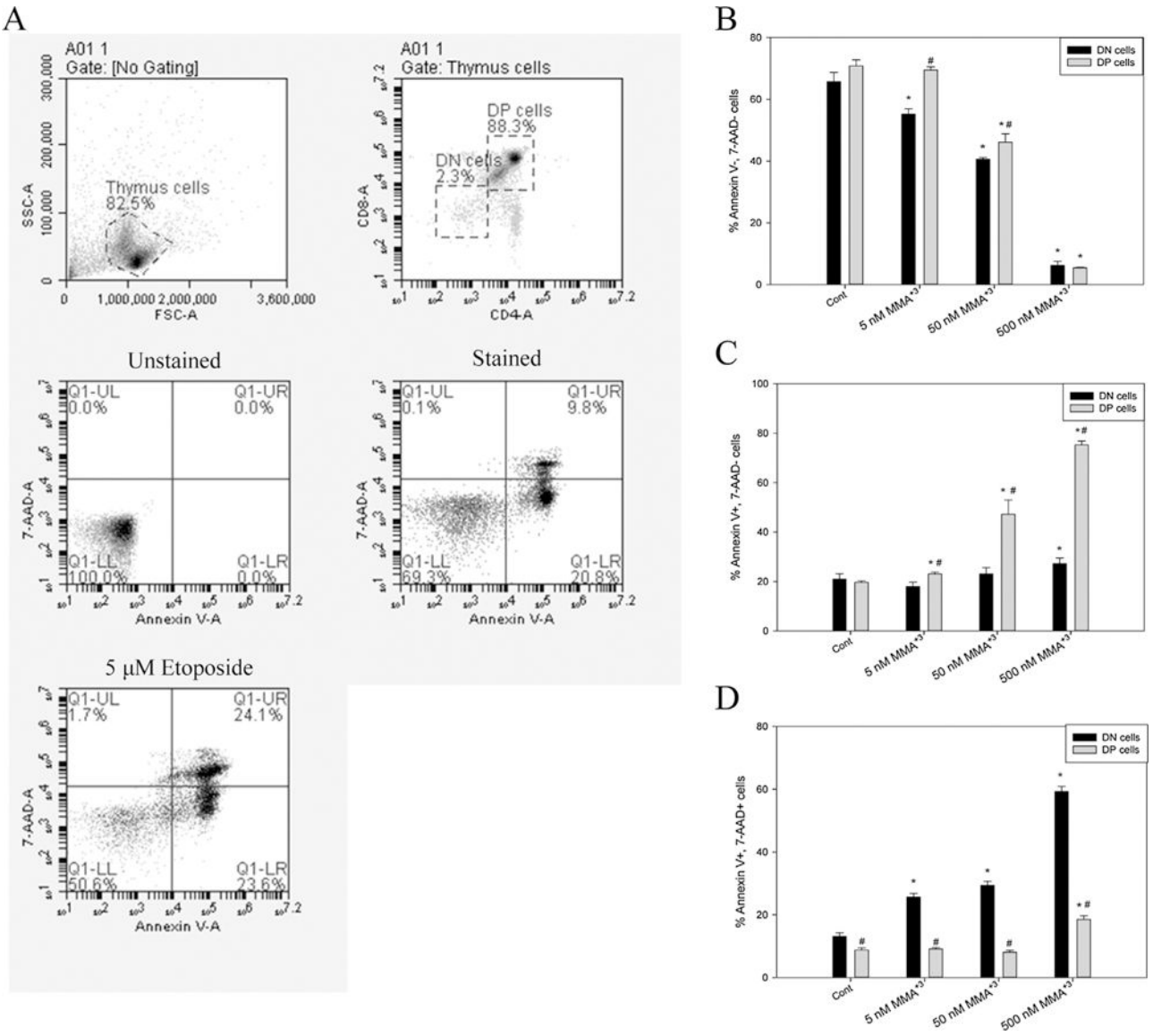

Fig. 4.

Apoptosis in DN and DP cells after exposure to 5, 50 and 500 nM MMA^{+3} for 18 h. Thymus cells were treated with MMA^{+3} and analyzed by CD4, CD8 cell surface markers and Annexin V/7-AAD staining. A, DN and DP cell gating, unstained, stained and positive controls.B,viable cells (Annexin V−, 7-AAD−). C, early apoptotic cells (Annexin V+, 7-AAD−). D, late apoptotic cells (Annexin V+, 7-AAD+). *Significantly different compared to Cont ($n = 3$, $p < 0.05$). # Significantly different compared to the DN cells at the same dose ($n = 3$, $p < 0.05$). Results are Means ± SD.

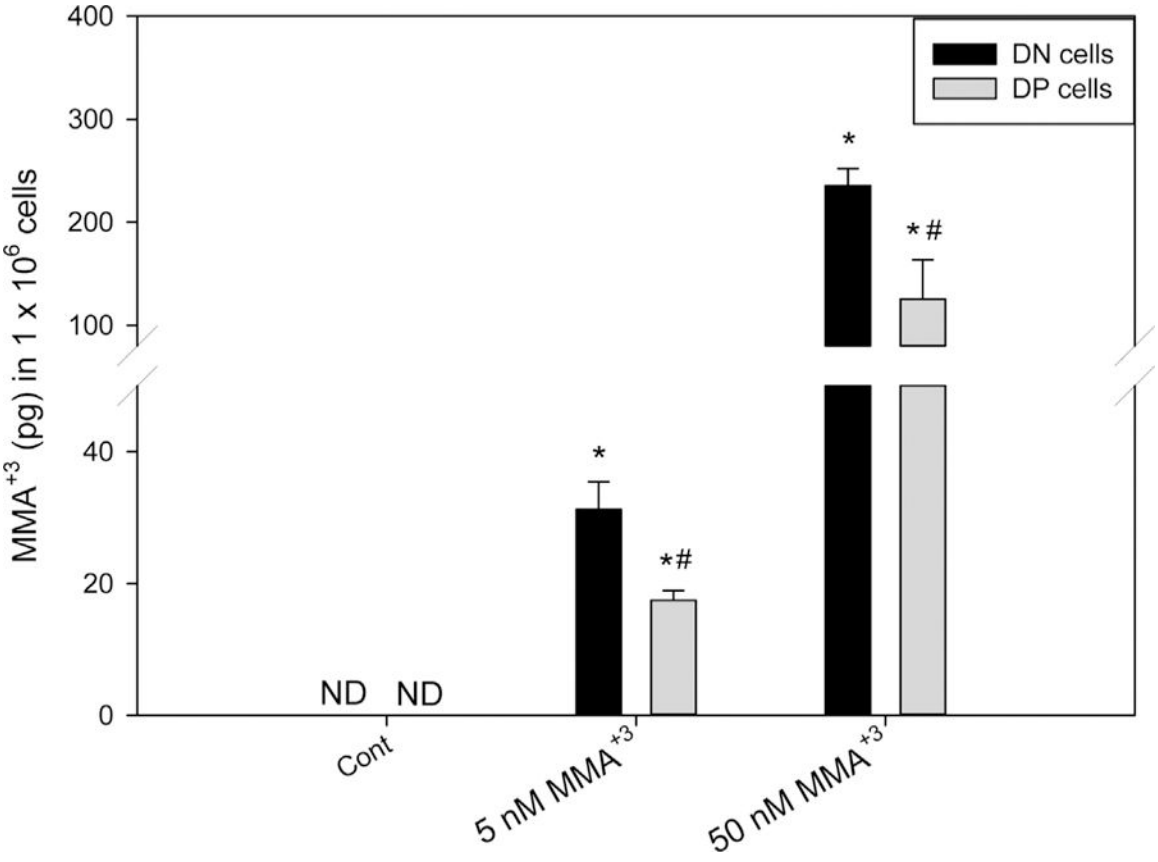

Fig. 5.

Intracellular MMA^{+3}levels in DN and DP cells treated with MMA^{+3} *in vitro* for 18 h. Sorted DN and DP were treated with MMA^{+3} for 18 h. Intracellular MMA^{+3}accumulation was measured by HG-CT-ICP-MS. ND, not detected. *Significantly different compared to Cont ($n = 3$, $p < 0.05$). # Significantly different compared to the DN cells at the same dose ($n = 3$, $p < 0.05$). Results are Means ± SD.